

# Lawrence Berkeley National Laboratory

## Lawrence Berkeley National Laboratory

### **Title**

Overview of Light-Ion Beam Therapy

### **Permalink**

<https://escholarship.org/uc/item/3qg6p5j4>

### **Author**

Chu, William T.

### **Publication Date**

2006-03-16

## Overview of Light-Ion Beam Therapy

William T. Chu\*

E.O. Lawrence Berkeley National Laboratory  
University of California, Berkeley

### History of Hadron Therapy

In 1930, Ernest Orlando Lawrence at the University of California at Berkeley invented the cyclotron. One of his students, M. Stanley Livingston, constructed a 13-cm diameter model that had all the features of early cyclotrons, accelerating protons to 80 keV using less than 1 kV on a semi-circular accelerating electrode, now called the "dee."<sup>1</sup> Soon after, Lawrence constructed the first two-dee 27-Inch (69-cm) Cyclotron, which produced protons and deuterons of 4.8 MeV. In 1939, Lawrence constructed the 60-Inch (150-cm) Cyclotron, which accelerated deuterons to 19 MeV. Just before WWII, Lawrence designed a 184-inch cyclotron, but the war prevented the building of this machine. Immediately after the war ended, the Veksler-McMillan principle of phase stability was put forward, which enabled the transformation of conventional cyclotrons to successful synchrocyclotrons. When completed, the 184-Inch Synchrocyclotron produced 340-MeV protons. Following it, more modern synchrocyclotrons were built around the globe, and the synchrocyclotrons in Berkeley and Uppsala, together with the Harvard cyclotron, would perform pioneering work in treatment of human cancer using accelerated hadrons (protons and light ions).

When the 184-Inch Synchrocyclotron was built, Lawrence asked Robert Wilson, one of his former graduate students, to look into the shielding requirements for of the new accelerator. Wilson soon realized that the 184-Inch would produce a copious number of protons and other light ions that had enough energy to penetrate human body, and could be used for treatment of deep-seated diseases. Realizing the advantages of delivering a larger dose in the Bragg peak<sup>2</sup> when placed inside deep-seated tumors, he published in a medical journal a seminal paper on the rationale to use accelerated protons and light ions for treatment of human cancer.<sup>3</sup> The precise dose localization provided by protons and light ions means lower doses to normal tissues adjacent to the treatment volume compared to those in conventional (photon) treatments.

---

\* Supported by the Director, Office of Science, Office of Basic Energy Sciences, of the U.S. Department of Energy under Contract No. DE-AC02-05CH11231.

<sup>1</sup> E.O. Lawrence and M.S. Livingstone, *Phys. Rev* **37**: 1707 (1931); and M.S. Livingston, "The Production of High-Velocity Hydrogen Ions Without the Use of High Voltages," PhD thesis, University of California, Berkeley (1931).

<sup>2</sup> W.H. Bragg and R. Kleeman, "On the ionization curves of radium." *Philosophical Magazine*, **8**: 726-738 (1904).

<sup>3</sup> R.R. Wilson, "Radiological use of fast protons," *Radiol.* **47**, 487-491 (1946).

Wilson wrote his personal account of this pioneering work in 1997.<sup>4</sup>

In 1954 Cornelius Tobias and John Lawrence at the Radiation Laboratory (former E.O. Lawrence Berkeley National Laboratory) of the University of California, Berkeley performed the first therapeutic exposure of human patients to hadron (deuteron and helium ion) beams at the 184-Inch Synchrocyclotron.<sup>5</sup> By 1984, or 30 years after the first proton treatment at Berkeley, programs of proton radiation treatments had opened at: University of Uppsala, Sweden, 1957<sup>6</sup>; the Massachusetts General Hospital-Harvard Cyclotron Laboratory (MGH/HCL), USA, 1961<sup>7</sup>; Dubna (1967), Moscow (1969) and St Petersburg (1975) in Russia<sup>8</sup>; Chiba (1979) and Tsukuba (1983) in Japan; and Villigen, Switzerland, 1984. These centers used the accelerators originally constructed for nuclear physics research. The experience at these centers has confirmed the efficacy of protons and light ions in increasing the tumor dose relative to normal tissue dose, with significant improvements in local control and patient survival for several tumor sites. M.R. Raju reviewed the early clinical studies.<sup>9</sup>

In 1990, the Loma Linda University Medical Center in California heralded in the age of *dedicated* medical accelerators when it commissioned its proton therapy facility with a 250-MeV synchrotron.<sup>10</sup> Since then there has been a relatively rapid increase in the number of hospital-based proton treatment centers around the world, and by 2006 there are more than a dozen commercially-built facilities in use, five new facilities under construction, and more in planning stages.

### Light-Ion Beam Therapy

In the 1950s larger synchrotrons were built in the GeV region at Brookhaven (3-GeV Cosmotron) and at Berkeley (6-GeV Bevatron), and today most of the world's largest accelerators are synchrotrons. With advances in accelerator design in the early 1970s, synchrotrons at Berkeley<sup>11</sup> and Princeton<sup>12</sup> accelerated ions with atomic numbers between 6 and 18, at energies that permitted the initiation of several biological studies.<sup>13</sup> It is worth noting that when the Bevatron was converted to accelerate light ions, the main push came from biomedical users who wanted to use high-LET radiation for treating human cancer.

---

<sup>4</sup> R.R. Wilson, "Foreword to the Second International Symposium on Hadrontherapy," in *Advances in Hadrontherapy*, (U. Amaldi, B. Larsson, and Y. Lemoigne, editors), Excerpta Medica, Elsevier, International Congress Series **1144**: ix-xiii (1997).

<sup>5</sup> C.A. Tobias, H.O. Anger and J.H. Lawrence, "Radiological use of high energy deuterons and alpha particles," *Am. J. Roentgenol. Radiat. Ther. Nucl. Med.* **67**: 1-27 (1952).

<sup>6</sup> B. Larsson, *Brit. J. Radiol.* **34**: 143-151 (1961).

<sup>7</sup> H.D. Suit, M. Goitein, J. Tepper, A.M. Koehler, R.A. Schmidt and R. Schneider, *Cancer* **35**: 1646-1657 (1975).

<sup>8</sup> L.L. Goldin, V.P. Dzhelepov et al., *Sov. Phys. Usp.* **16**: 402 (1973).

<sup>9</sup> M.R. Raju, "The History of Ion Beam Therapy," in *Ion Beams in Tumor Therapy* (Ute Lintz, ed.), Chapman & Hall, 3-9 (1995).

<sup>10</sup> J.M. Slater, J.O. Archambeau, D.W. Miller, M.I. Notarus, W. Preston, and J.D. Slater, "The proton treatment center at Loma Linda University Medical Center: rationale for and description of its development," *Int J Radiat Oncol Biol Phys.* **22**: 383-389 (1992).

<sup>11</sup> H.A. Grunder, W.D. Hartsough and E.J. Lofgren, *Science* **174**: 1128-1129 (1971).

<sup>12</sup> M.G. White, M. Isaila, K. Predec and H.L. Allen, *Science* **174**: 1121-1123 (1971).

<sup>13</sup> C.A. Tobias, *Radiology* **108**: 145-158 (1973).

## Physical Characteristics of Light-Ion Beams

### Bragg Peak and Spread-Out Bragg Peak

When energetic light ions enter an absorbing medium, they are slowed down by losing their kinetic energy mainly through ionizing the medium. The energy loss per unit mass for unit area of the absorber, or specific ionization (usually expressed in keV/ $\mu\text{m}$  in water) increases with decreasing particle velocity, giving rise to a sharp maximum in ionization near the end of the range, known as the Bragg peak. When a beam of monoenergetic heavy charged particles enters the patient body, the depth-dose distribution is characterized by a relatively low dose in the entrance region (plateau) near the skin and a sharply elevated dose at the end of the range (Bragg peak), viz., Fig. 1(a). A pristine beam with a narrow Bragg peak makes it possible to irradiate a very small, localized region within the body with an entrance dose lower than that in the peak region.<sup>14</sup> To treat an extended target, the Bragg peak is spread out to cover volume by modulating the energy of the particles to form a spread-out Bragg peak (SOBP), viz., Fig. 1(b).

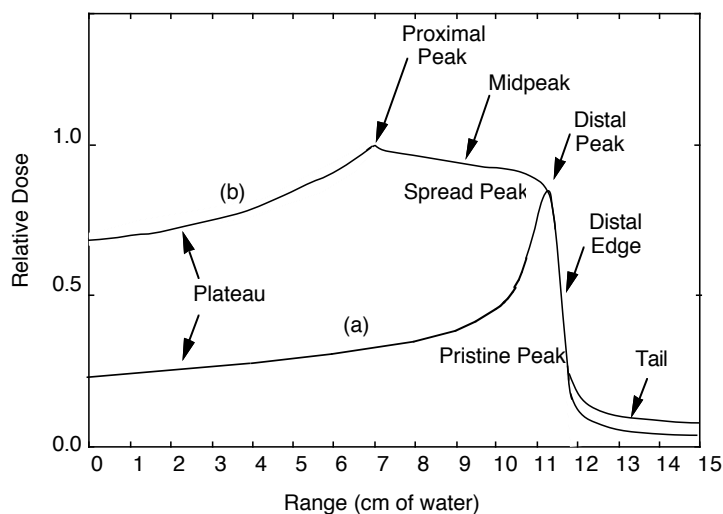


Fig. 1. (a) Bragg curve of an ion beam. (b) SOBP curve, which has several regions referred to as the plateau, the proximal peak, the midpeak, the distal peak regions, the distal dose-falloff edge, and the tail. A uniform biological dose distribution within the SOBP region is obtained by compensating for the variation in RBE of the radiation as a function of penetrating depth.

Examples of SOBP ionization curves, adjusted with RBE, of several ion beams are shown in Fig. 2. For the light-ion beams, the radiation dose abruptly decreases beyond the Bragg peak, sparing any critical organs and healthy tissues located downstream of the target volume from unwanted radiation. The entrance dose, the dose upstream of the target, is also low compared with the peak dose.

<sup>14</sup> C. A. Tobias, H. O. Anger and J. H. Lawrence, Am. J. Roentgenol. **67**: 1-27 (1952).

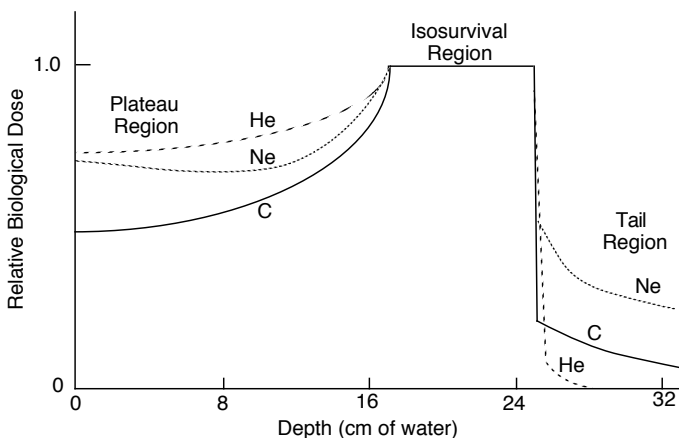


Fig. 2. The relative *biological* doses of SOBPs of helium, carbon, and neon ion beams as a function of penetrating depth in water are shown for comparison. The doses are normalized at the isosurvival region and the figure shows the different relative entrance, plateau, and tail doses for these beams.

### Multiple Scattering and Range Straggling

*Multiple* scattering of an incident ion stems from the small angle deflection of it due to collisions with the nuclei of the traversed material. Numerous small angle deflections in an ion beam lead to lateral spreading of the incident ions away from the central trajectory resulting in larger divergence of the beam. Elastic Coulomb scattering dominates this process with a small strong-interaction scattering correction. The angular distribution of the scattered particles is roughly Gaussian for small deflection angles, and the mean beam deflection is approximately proportional to the penetration depth (Fig. 3(B))

*Range straggling* is the dispersion of the path length of a particle beam due to statistical fluctuations in the energy-loss process. The end result is to produce a smearing of the range of the stopping particle beam. For a particle traveling in a direction  $X$ , with energy  $E$  and mean range  $R$ , the distribution of ranges,  $s(x)$ , is Gaussian,<sup>15</sup>

$$s(x) = \frac{1}{\sqrt{2\pi}\sigma_x} e^{-(x-R)^2/2\sigma_x^2}$$

In the region where this formula is valid ( $2 < R < 40$  cm),  $\sigma_x$  is almost proportional to range,  $R$ , and inversely proportional to the square root of the particle mass number,  $A$ .

Multiple scattering and range straggling effects for ion beams vary approximately inversely to the square-root of the mass of the particle. Interactions of several light ions penetrating absorbing material is characterized in Fig. 3, showing  $\sigma$  for range straggling (A) and mean beam deflections due to multiple scattering (B). Removing material from the beam line could minimize the range straggling and multiple scattering. For example magnetic deflection can eliminate the material needed to spread the beam in a scattering system, or changing the accelerator energy can eliminate material degraders used to change the energy of the beam.

<sup>15</sup> H. W. Lewis, Phys. Rev. **85**: 20 (1952).

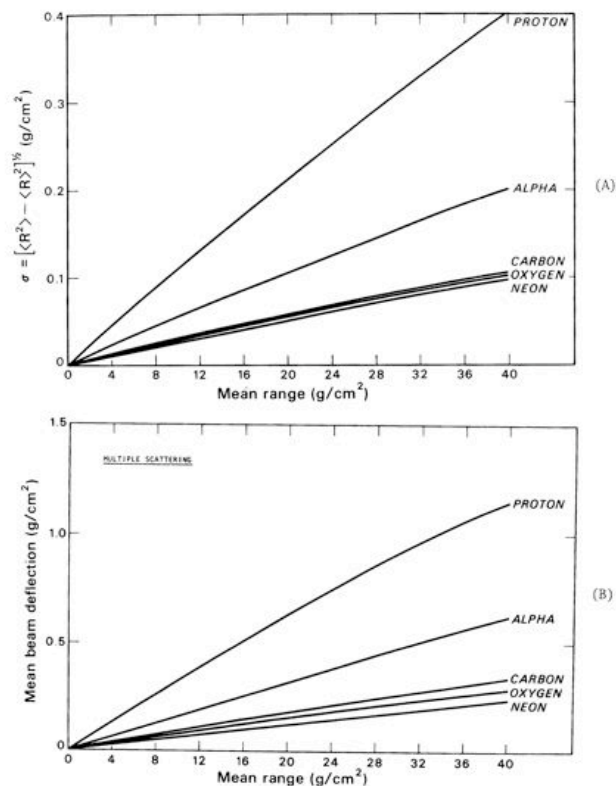


Fig. 3. Interactions of light ions penetrating absorbing material are characterized by  $\sigma$  for range straggling (A) and for multiple scattering (B). For example, the  $\sigma$  values for range straggling in 20-cm of water are: 2.0, 1.0, 0.6, and 0.5 mm for protons, helium, carbon, and neon ions, respectively.

The sharpness of the lateral dose falloff, often called the *apparent* penumbra, is of clinical importance because the radiation exposure of the normal tissues adjacent to the target volume often limits the therapy dose. Heavier ion beams exhibit sharper lateral dose falloffs at the field boundary than for the lighter ions: viz., Fig. 4 that compares the penumbrae of proton and carbon beams. The penumbra width increases essentially linearly with the penetration depth of the beam. For low-Z ions, such as protons, sharpest dose falloffs are obtained when the final collimator is at the surface of the patient. For higher-Z ion beams, such as carbon ion beams, scanning narrow pencil beams without collimations will produce narrow penumbrae.

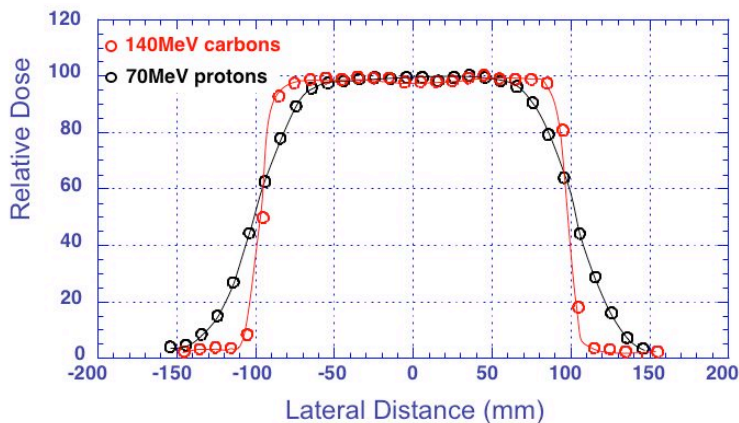


Fig. 4. The penumbra of a carbon beam is much sharper than that of a proton beam of the comparable range. (Based on the paper presented by H. Tsuji, at the 39<sup>th</sup> meeting of PTCOG, San Francisco, October 2002.)

The effect of multiple scattering becomes more pronounced for small size beams as indicated in Fig. 5, which examines depth-dose curves of proton and carbon-ion beams of comparable range for an uncollimated beam and a 1-cm diameter collimated beam. The Bragg peaks appear almost unchanged for the two carbon-ion beams; whereas, the Bragg peak is much suppressed for the collimated proton beam (Fig. 5(a)). Lateral dose distributions of the collimated 1-cm diameter proton beam exhibits broader penumbra, especially at the end of its range and wider range straggling. The collimated carbon-ion beam shows much smaller beam scattering and straggling. For treating small targets, where the sharpness of the lateral dose falloff is essential, the choice of the heavier ion beam becomes important.<sup>16</sup>

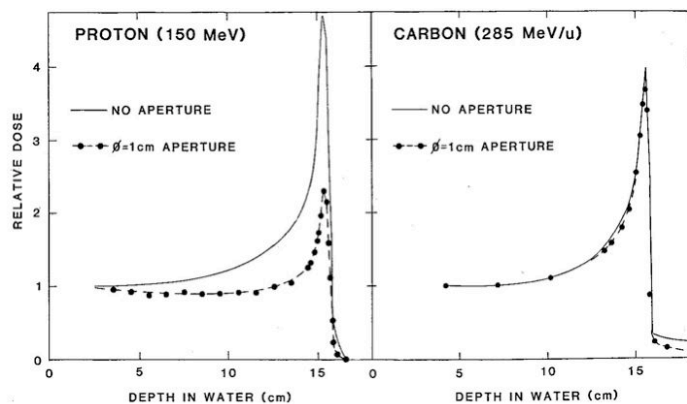


Fig. 5(a). Depth-dose curves of proton and carbon-ion beams of comparable range are compared. For each ion, uncollimated and collimated 1-cm diameter beams are examined. Bragg peaks appear almost unchanged for the two carbon-ion beams; whereas, the Bragg peak is much suppressed for the collimated proton beam.

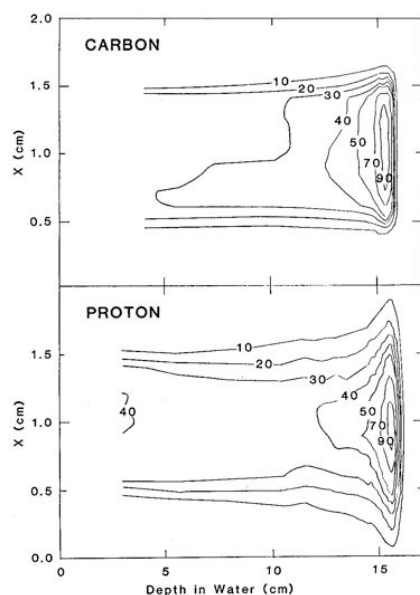


Fig. 5(b). Dose distributions in the plane that includes the central ray of proton and carbon-ion beams are shown. Both beams are collimated to a 1-cm diameter.

<sup>16</sup> M.H. Phillips, K.A. Frankel, J.T. Lyman, J.I. Fabrikant and R.P. Levy, *Int. J. Radiat. Oncol. Biol. Phys.* **8**: 211-220 (1990).

## Beam Fragmentation

As a particle beam penetrates through matter, the primary particles suffer fragmentation collisions, which decrease the number of primaries with the corresponding increase of lighter fragments along the penetration path.<sup>17</sup> Fragmentation refers to the process where the projectile nucleus, after suffering a nuclear collision with a target nucleus, is broken apart into several daughter particles. The remnants of the projectile nucleus emerge from the absorbing material with similar speeds as that of the original projectile nucleus. The target nucleus may also break apart, but these fragments have relatively low energy and do not travel with the beam.

Fig. 6 shows the measured fragment number and dose contribution as a function of the particle charge for a neon-ion beam after traversing 16 cm of water. The measurement was made with BERKLET. The instrument consists of a 300- $\mu\text{m}$  thick Si detector and a 5.5-cm thick Ge detector, which when operated in coincidence, measures the  $dE/dx$  and the total energy of the particle, respectively.<sup>18</sup>

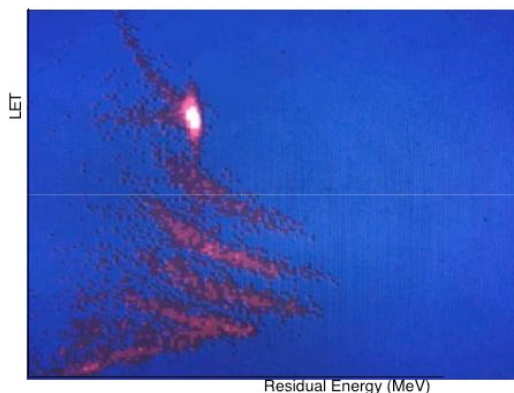


Fig. 6(a). Scatter plot of fragments on the residual energy versus LET (or  $dE/dx$ ). The brightest spot is the primary beam particles. The bands are particles of a given charge. (CBB 875-4105)

<sup>17</sup> A.S. Goldhaber and H.H. Heckman, *Ann. Rev. Nucl. Part. Sci.* **28**: 161-205 (1978).

<sup>18</sup> J. Llacer, J.B. Schmidt and C.A. Tobias, *Med. Phys.* **17**: 158-162 (1990); and J. Llacer and H.W. Kraner, *Nucl. Instrum. and Methods* **98**: 467-475 (1972).



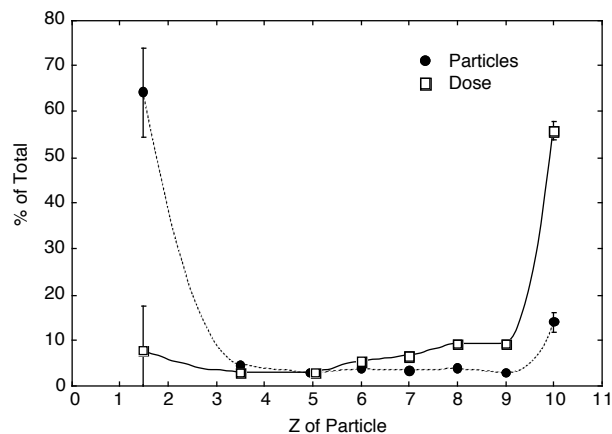


Fig. 6(b). Two sets of data show contributions of different atomic charges to the total particle number and the total dose delivered. Fragments are from neon ions in the proximal peak region of a 12-cm spread out Bragg peak with a residual range of 28 cm in water. It corresponds to the beam traversing 16 cm of water. The data for low  $Z$  values (1-2 and 3-4) are lumped together.

For protons colliding with a water-like target material (e.g., soft tissue), knocked-out neutrons from the target nuclei are the dominant interaction products. These neutrons contribute to the dose delivered beyond the stopping region of the primary projectile. Light ions also produce such a neutron background. Even after accounting for the higher RBE of the neutrons produced, they contribute less than 0.5 % of the biological dose delivered to the patient.<sup>19</sup> Their contribution would be larger in cases where the range of the beam is severely degraded upstream of the patient, such as by a double scattering method, then whole body exposure could become an issue.

As discussed above, carbon and neon ions fragment into a larger number of nuclear species. These fragments lead to a significant dose beyond the actual stopping range of the primary particles, and contribute significantly to the dose within the spread-out Bragg peak. In general, the heavier the nuclear projectile, the larger the dose delivered in the region beyond the Bragg peak when normalized to the dose delivered by primary ions at the proximal peak of the SOBP.

An additional complication is that a fragmented beam has a radiobiological effect different from that of the primary beam. The LET distribution of the fragmented beam becomes quite complex as more of the primary beam fragments<sup>20</sup>; hence, RBE, which is a function of the LET of the beam, is a function of the depth of the material penetrated. For SOBP, the composition of the beam and its biological effect is also a function of depth and must be accounted by adjusting the physical depth-dose distribution to obtain a uniform biological dose distribution.

### Biological Rationale for Clinical Use of Light Ions

By the late 1980s, radiobiological research with light-ion beams, essential concomitant to a successful and safe clinical research program, had three major aspects. First was determining the optimal strategies for tumor treatment by analysis of the biological responses of tumor tissue to different ions, delivered at various doses and at various intervals. Second, determining tolerance doses and the risks of carcinogenesis and cell transformation for normal tissues. Thirdly, fundamental radiobiological understanding and characterizing physical phenomena

<sup>19</sup> J.B. McCaslin, P.R. LaPlant, A.R. Smith, W.P. Swanson and R.H. Thomas, IEEE Trans. Nucl. Sci. **NS-32**: 3104-3106 (1985).

<sup>20</sup> J. Llacer, C.A. Tobias, W.R. Holley and T. Kanai, Med. Phys. **11**: 266-278 (1984).

such as ion fragmentation and biological effects such as DNA damage and repair. Knowledge gained from basic research influenced the choices of ion, energy, beam delivery system, and treatment schedule. At the same time, the emerging picture of the processes by which radiation causes genetic damage, and by which the DNA attempts to recover from the insult, enhanced our understanding of the risks posed by radiation exposure in general, including exposure associated with radiation accidents and space exploration, as well as radiotherapy.

These early studies are sometimes called “classical” cellular radiobiology to distinguish it from “new” molecular radiobiology that was developed in more recent years.<sup>21</sup> We will describe here some of the significant results that have emerged from early radiobiological research at Berkeley, especially as they relate to then ongoing cancer therapy trials.

### **LET, OER and RBE**

The higher relative biological effectiveness (RBE) values of higher-Z ion beams indicated a high likelihood of an enhanced therapeutic potential when compared with lower-Z particle beams, such as protons.<sup>22</sup> The RBE of each ion has been studied in some detail with a variety of biological endpoints showed that the RBE of an ion beam is not a simple function of LET even though LET is usually used to describe of the differences in radiation damage by various light ions (Fig. 7(a)).<sup>23</sup> RBE also depends on the endpoint of measurements, such as the survival level, the kinds of ions and types of cells and tissues used in the experiments (Fig. 7(b)). In general, the values of RBE and the degrees of dose localization increases with the Z values from protons to silicon ions, and at LET values higher than approximately 200 keV/μm, the RBE values decline.

Another important point is that the failures in local control of tumors treated with low-LET radiation (conventional and proton radiation) are often due to its inability to completely eradicate anoxic tumor cells which are resistant to such radiation. High-LET radiation exhibits the biological advantages of lower oxygen effect (lower OER values), as indicated in Fig. 8. The OER value is defined as the ratio of the dose needed to render the same end-point for anoxic cells to that for well-oxygenated cells.

---

<sup>21</sup> J. Yarnold, “Molecular and cellular responses to radiotherapy,” in *Advances in Hadrontherapy*, (U. Amaldi, B. Larsson, and Y. Lemoigne, editors), Excerpta Medica, Elsevier, International Congress Series **1144**: 3-11 (1997).

<sup>22</sup> *PART III. “Particles and Radiation Therapy, Third International Conference,”* Int. J. Radiat. Oncol. Biol. Phys., **8** (1982).

<sup>23</sup> E. A. Blakely, F. Q. H. Ngo, S. B. Curtis and C. A. Tobias, *Adv. Radiat. Biol.* **11**: 295- 389 (1984).

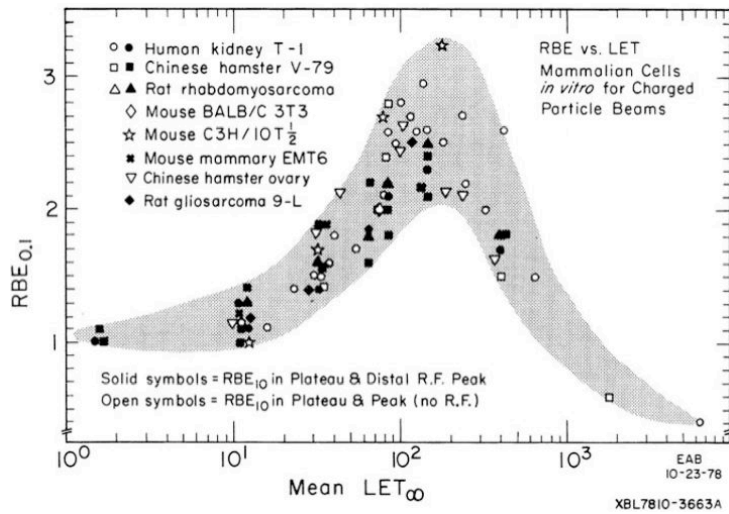


Fig. 7(a). RBE vs. LET. The data is from a number of experiments using a number of ions, energies and cell types. The shaded area shows the general trend of the data.

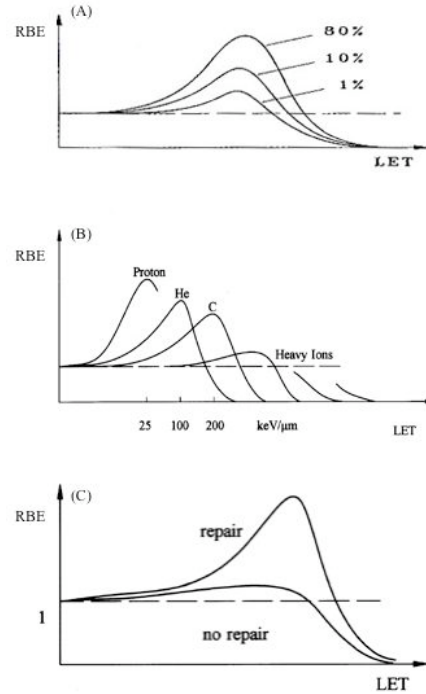


Fig. 7(b). The relationship between RBE vs. LET is a function of (A) the endpoint of measurements, e.g., survival, (B) kinds of ions, and (C) type of cells or tissues.

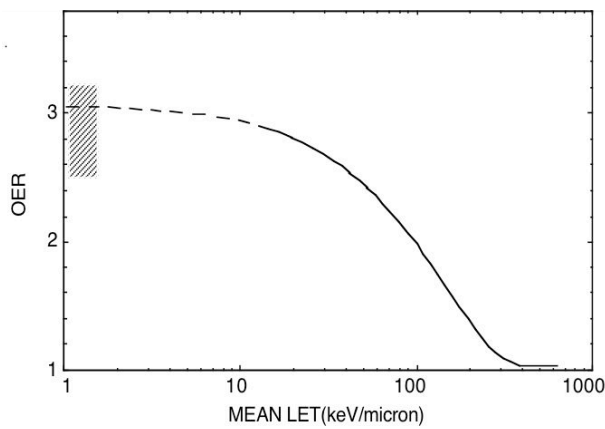


Fig. 8(a). OER vs. LET. The shaded area represents the measured OER for x rays. The curve is a generalized fit to data using various ions and energies.

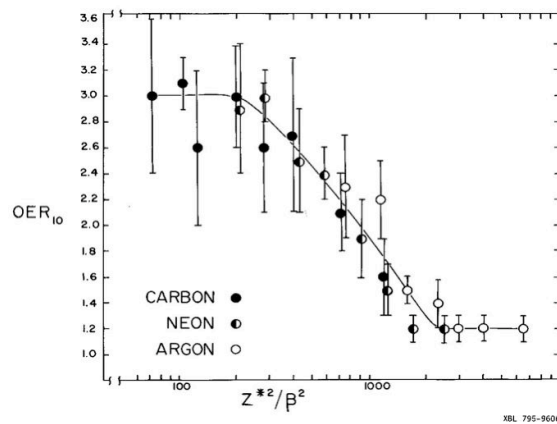


Fig. 8(b). Measured data of OER vs.  $Z^2/\beta^2$  for carbon, neon and argon ion beams.

In 1967, Tobias and Todd gave the scientific justification for utilizing light-ion beams combining the characteristics of light-ion beams in LET, RBE and OER.<sup>24</sup> In 1980 LBNL published a report compiling the results of research in physics, biology and medicine about light-ion therapy.<sup>25</sup> The conjecture was that, referring to Fig. 9, the most advantageous species of ions for cancer treatment are located at higher values of “oxygen gain factor,” which is a parameter proportional to the inverse of OER, and at the same time at higher values of RBE. For the smaller and shallower targets (upper panel), it appeared that carbon and neon-ion beams are superior to other ions. For larger and deeper targets (lower panel), the relative placement of each of the therapy modalities is altered, and proton, helium and carbon-ion beams are quite similar.

One has to carefully interpret the meanings of Fig. 9 under other clinical considerations. Simple mindedly, we may take RBE not crucial on the assumption that the low RBE may be readily compensated with higher physical doses; whereas, the oxygen gain factor is biologically important factor that is intrinsic properties of the ion species. However, the gain in oxygen effect must be weighed against the increased mutagenesis and carcinogenesis of the higher-Z ions. It was generally agreed that ions of atomic numbers between carbon and silicon are the most interesting high-LET ions for clinical use.<sup>26,27</sup> Today, carbon ion beams are chosen for therapy as the carbon ion has both biological and dose localization advantages superior to those of lighter ions such as protons, yet avoids some complications with higher-Z ions. For carbon ion beams, enough high LET is present to provide significant differences in DNA damage, and suppression of radiation repair. The use of heavier ions such as neon and silicon leads to complexity in treatment planning because of the high LET in the entrance region and the fragment tail. Normal tissues in these regions need to be carefully assessed and treatment plans designed which avoid significant late effects, especially in CNS.

The radiobiological rationale for using these high-Z ions for therapy,<sup>28,29</sup> as understood then, can be summarized as follows: (a) The high resistance of hypoxic cells relative to oxic cells is reduced when irradiated with high-LET radiation. (b) Slowly proliferating cells (in  $G_0$  or long  $G_1$  phase in cell cycle) show a similar increase in sensitivity, if irradiated with high-LET radiation. (c) Overall treatment time with high-LET radiation can be shortened since fewer fractions of larger doses may be used instead of multiple fractions of small doses when the surrounding normal tissue damage in a fewer fraction can be kept comparable to that of a standard low-LET fraction. The last point squarely contrasts against the rationale that there is an

---

<sup>24</sup> C. A. Tobias and P. W. Todd, Radiobiology and Radiotherapy, Natl. Cancer Inst. Monogr. 24: 1-21 (1967).

<sup>25</sup> “Biological and Medical Research with Accelerated Heavy Ions at the Bevalac, 1977-1980,” (M.C. Pirruccello and C.A. Tobias, eds.), Lawrence Berkeley Laboratory, LBL-11220, pp. 423 (1980).

<sup>26</sup> E.A. Blakely, C.A. Tobias, B.A. Ludewigt, and W.T. Chu, “Some Physical and Biological Properties of Light Ions,” *Proc. of the Fifth PTCOG Meeting and the International Workshop on Biomedical Accelerators, December 1986* (ed. by W. T. Chu), Lawrence Berkeley Laboratory, Berkeley, CA, LBL-22962, 19-41 (1987).

<sup>27</sup> P.K. Lillis-Hearne, J.R. Castro, “Indications for Heavy Ions- Lessons from Berkeley,” in *Ion Beams in Tumour Therapy* (V. Linz, ed.), Chapman & Hall, 133-141 (1995).

<sup>28</sup> J.F. Fowler, *Nuclear Particles in Cancer Treatment*, Medical Physics Handbook, **No. 8**, Adam Higler Press, Bristol, England (1981).

<sup>29</sup> E. J. Hall, *Int. J. Radiat. Oncol. Biol. Phys.* **8**: 2137-2140 (1982).

advantage in using multiple, small fractions of low-LET radiation for sparing late damage.<sup>30</sup> Cutting down the number of ion-beam treatments would benefit individual patients as well as the management of the clinic.

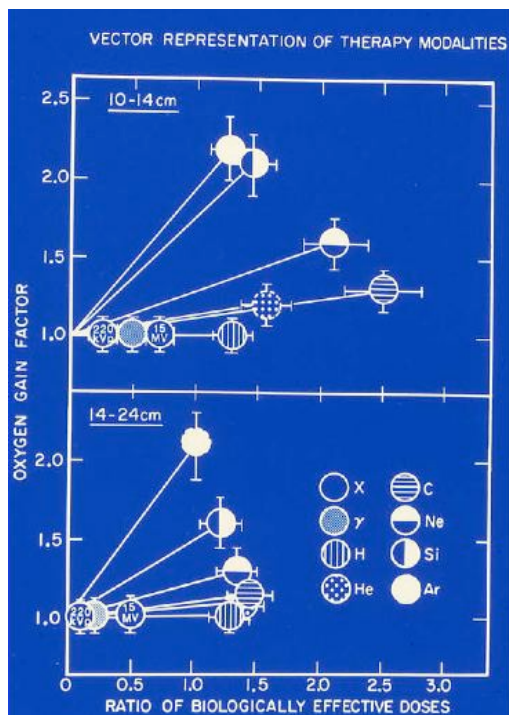


Fig. 9. "Vector representation" of therapy modalities for treatment of: small shallow targets (upper panel) and large deep targets (lower panel). The "oxygen gain factor" is a parameter proportional to the inverse of OER, and the "ratio of biologically effective doses" represent RBEs of the ions in question. (XBL 808-36238)

### Physical Parameters of Clinical Beams

Protocols for heavy charged-particle beam dosimetry have been established by the American Association of Physicists in Medicine for protons and heavier ions.<sup>31</sup> They describe the methods of calculating the dose based on measurements using various dosimeters. Discussions of these methods are reviewed in other publications.<sup>32</sup>

### RBE and LET Distributions

The main function of the treatment planning and delivery is to create a radiation field that produces uniform cell killing or a uniform biological response. Changes in the primary

<sup>30</sup> H.D. Suit, M. Goitein, J.E. Munzenrider, L. Verhey, P. Blitzer, E. Gragoudas, A.M. Koehler, M. Urie, R. Gentry, W. Shipley, M. Urano, J. Duttonhaver and M. Wagner, *Int. J. Radiat. Oncol. Biol. Phys.* **8**: 2199-2205 (1982).

<sup>31</sup> *American Association of Physicists in Medicine, Protocols for Heavy Charged Particle Beam Dosimetry, A Report of Task Group 20, Radiation Therapy Committee, American Institute of Physics, New York, AAPM Report No. 16* (1986).

<sup>32</sup> J. J. Broerse, J. T. Lyman and J. Zoetelief, "Dosimetry of External Beams of Nuclear Particles," in *The Dosimetry of Ionizing Radiation* (ed. by K. R. Kase, B. E. Bjärngard and F. H. Attix), Academic Press, Orlando, FL, **Vol. I**: 230-290 (1985).

particle beam from fragmentation lead to changes in the biological effectiveness of the radiation. Fig. 10 shows a measurement of RBE as a function of depth. Dose-averaged LET,  $L_D$ , is defined as:

$$L_D = \frac{\int L D(L) dL}{\int L \Phi(L) dL}$$

where  $D(L)$  is the dose contributed by particles of a given LET,  $L$ , and  $\Phi(L)$  is the fluence of particles with the given  $L$ , and

$$D(L) = \frac{1.6 \times 10^7 \Phi L}{\rho},$$

where  $\rho$  is the material density in  $\text{g/cm}^3$ ,  $L$  is measured in  $\text{keV}/\mu\text{m}$  and  $\Phi$  in  $\text{particles/cm}^2$ .

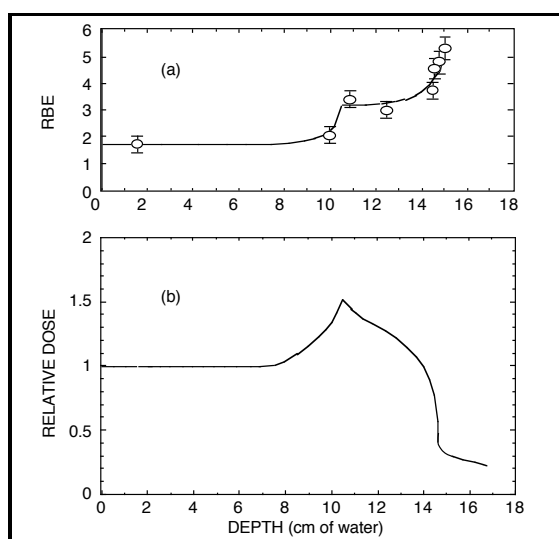


Fig. 10(a) Measured RBE data at various depths in water of a range-modulated beam. The solid line is to guide the eye.

(b) The associated physical dose distribution, which would render an isosurvival region in SOBP when the physical dose is multiplied by RBE at each depth.

The tail region of the depth-dose curve is a complex mix of particles; its RBE is important in predicting the response of tissue beyond the Bragg peak where critical structures might be found. Tail doses are typically one tenth of the dose in the proximal peak, and biological measurements in the tail region are difficult due to the large dose need at the proximal peak in order to measure reliably cell responses in the tail. Measurements of dose-averaged LET in this region are simpler to make, but not very straightforward in predicting the biological effects.

### Verification of Treatment planning and Delivery Using Radioactive Beams

Treatment plans and delivery usually rely on xCT data, where the CT numbers are calibrated for ion beam stopping power in various types of tissues (see Fig. 11).<sup>33</sup> Such treatment plans

<sup>33</sup> G. T. Y. Chen, "CT in high LET therapy planning," *Proc. of the Symposium on Computed Tomography in Radiotherapy, September 1981* (ed. by C. C. Ling and R. Morton), Washington, DC, Raven Press, New York, 221-228 (1983).

could render errors as large as  $\pm 5$  mm in a 10 cm range.<sup>34</sup> For ion-beam treatment, the penalty paid for a small range inaccuracy is much more severe than for photon treatment as schematically illustrated in Fig. 12. By substituting a radioactive beam to deliver a “treatment” according to a therapy plan, and imaging the actual treatment volume, the conformation of the delivered dose with the target volume can be verified.<sup>35,36</sup>

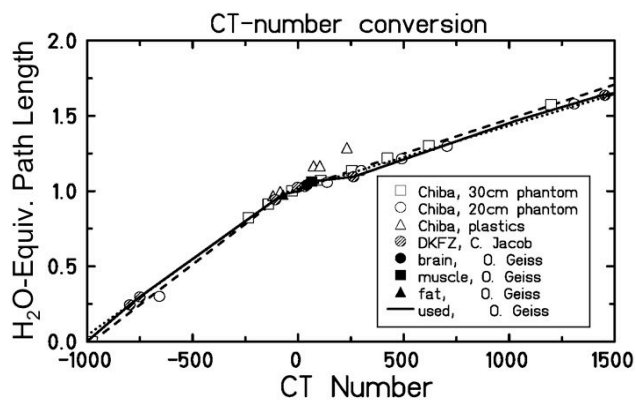


Fig. 11. Conversion of the CT numbers of tissues to water-equivalent path lengths for ion-beam treatment planning.

When a stable nucleus of an ion beam collides with a nucleus of the target material, the two nuclei knock off pieces (nucleons) of one another in peripheral collisions. Projectile ions may emerge, with one or two neutrons knocked out, with approximately the same velocity. The radioactive secondaries can be separated from the primary ion beam by magnetic momentum analysis and collected, and transported from the production target to the treatment room, and into the patient body. Production and collection of radioactive beams such as  $^{19}\text{Ne}$  produced from  $^{20}\text{Ne}$  and  $^{11}\text{C}$  and  $^{10}\text{C}$  from  $^{12}\text{C}$  have been investigated at LBNL.<sup>37</sup> The most interesting isotope is  $^{10}\text{C}$  (positron emitter, 19 second half life) as it is suitable for PET imaging. If the Bragg peak of a  $^{10}\text{C}$  beam of known momentum were aligned to the distal edge of a target volume inside the patient body, one can deliver with confidence a  $^{12}\text{C}$  beam into the same target.

<sup>34</sup> E. L. Alpen, W. Saunders, A. Chatterjee, J. Llacer, G. T. Chen and J. Scherer, *Brit. J. Radiol.* **58**: 542-548 (1985).

<sup>35</sup> J. Llacer, *Nucl. Sci. Applications* **3**: 111 (1988)

<sup>36</sup> S. D. Henderson, M. Collier, T. Renner, A. Chatterjee and J. Llacer, *Med. Phys.* **14**: 468 (1987).

<sup>37</sup> J. R. Alonso, B. Feinberg, J. G. Kalnins, G. F. Krebs, M. A. McMahan and I. Tanihata, "Radioactive beam production at the Bevalac," *Proc. of the First International Conference on Radioactive Nuclear Beams, Berkeley, CA, October 16-18, 1989* (ed. by W. D. Myers, J. M. Mitschke and E. B. Norman), World Scientific Publishing Co., Teaneck, NJ, 112 (1990).

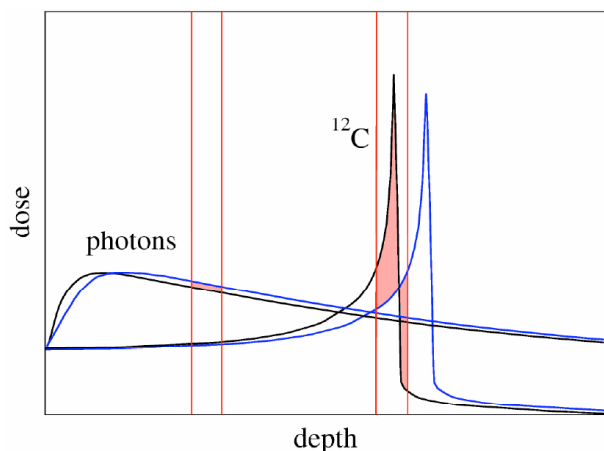


Fig. 12. For photon treatment, an error in target depth, indicated by two red lines at left, results in small dose error (red area). Whereas, for light ions, a similar error in range determination, shown in displaced Bragg peaks, would result in much more severe dose error as indicated by red areas (a big under-dose under the peak, and an overdose beyond the dose falloff region).

A schematic drawing of a specially-developed PET detector, called “Positron Emitting Beam Analyzer (PEBA) is shown in Fig. 13(a). It illustrates how PEBA localizes a stopping radioactive (positron-emitting) nucleus by measuring the annihilation photons of the positron emitted by the decay of  $^{10}\text{C}$  nuclei. The transverse dimension of the stopping region of the  $\text{C}^{10}$  nuclei and distance between the stopping nucleus and the point of annihilation are greatly exaggerated in Fig. 13(a). A PET image of stopping  $^{19}\text{Ne}$  in a phantom is shown in Fig. 13(b). One can determine the location of the Bragg peak within  $<0.5$  mm using sophisticated PET systems.

In a similar vein, GSI has implemented a PET system for in-beam in-situ therapy control, i.e., during ion beam treatment by assessing the radioactive isotopes produced by the  $^{12}\text{C}$  beams.<sup>38</sup>

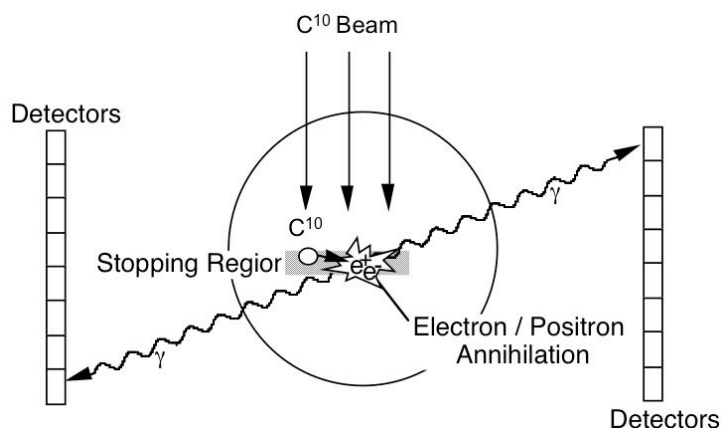


Fig. 13(a). A schematic drawing of PEBA.

<sup>38</sup> W. Enghardt, J. Debus, T. Haberer, B.G. Hasch, R. Hinz, O. Jakel, M. Kramer, K. Lauckner, J. Pawelke, “The application of PET to quality assurance of heavy-ion tumor therapy,” *Strahlenther Onkol.* **175 Suppl. 2:** 33-36 (1999)



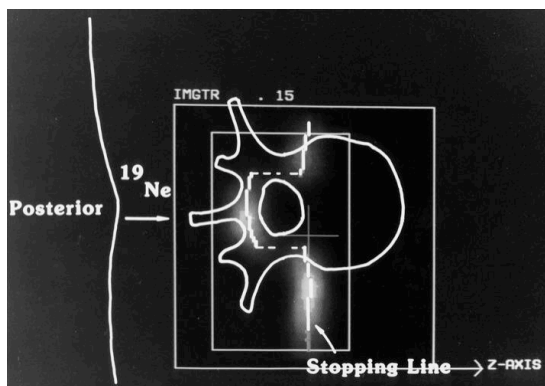


Fig. 13(b). An image of the stopping region of  $^{19}\text{Ne}$ . The beam was created by a compensator to exclude the spinal cord region of a patient (phantom) from the Bragg peak radiation. (XBC 865-4162)

### Ion Beam Research for Space Biology

Beyond the protection of the Earth's magnetic shield, the abundance of galactic cosmic rays, both light and heavy ions, is such that during a three-year trip to Mars 30% of the cell nuclei in an astronaut's body would be traversed by one or more heavily ionizing particles ( $10 \leq Z \leq 28$ ), assuming shielding typical of today's spacecraft. Iron nuclei are the major contributor to these radiation effects, but their consequences must be understood. Radiobiology research in light-ion therapy naturally extended into space biology research program, first at the Bevalac at LBNL and now at the Booster Accelerator Facility of the Relativistic Heavy Ion Collider (RHIC) at the Brookhaven National Laboratory. It focuses on the effects of both iron-ion beams and the secondary particles produced by fragmentation in absorbing materials.<sup>39</sup> Experiments are in progress to determine their effects on cell inactivation and neoplastic cell transformation and to calculate the cross sections for cell transformation by low- and high-LET radiation. Preliminary results indicate that, compared with the cross section for cell inactivation or death, the cross section for cell transformation is about 10,000 times smaller. Such a difference implies that only a very few genes are involved in radiation-induced cell transformation. Life shortening, cataract formation, and tumorigenesis in animals irradiated with iron-ion beams are also under investigation. Early results on cataract expression suggest a shortened latency for iron-ion exposure, compared with low-LET radiation.

### Clinical Trials Using Light Ions

The construction of the Bevalac accelerator complex at LBNL, in which the SuperHILAC injected ion beams into the Bevatron, expanded the opportunity for medical studies with light ion beams.<sup>40</sup> J.R. Castro and his team conducted clinical trials for treating human cancer using light ion beams at the 184-Incg Synchrocyclotron and the Bevalac from 1977 to 1992, when the

<sup>39</sup> TASK GROUP ON THE BIOLOGICAL EFFECTS OF SPACE RADIATION. *Radiation Hazards to Crews of Interplanetary Missions: Biological Issues and Research Strategies*. Washington, DC. Space Studies Board Commission on Physical Sciences, Mathematics and Applications, National Research Council. National Academy Press (1996).

<sup>40</sup> A. Ghiorso, H. A. Grunder, W. Hartsough, G. Lambertson, E. Lofgren, K. Lou, R. Main, R. Mobley, R. Morgado, W. Salsig and F. Selph, IEEE Trans. Nucl. Sci. **NS-20**: 155 (1973).

accelerators were closed.<sup>41</sup> Ions of interest ranged from  $^4\text{He}$  to  $^{28}\text{Si}$ .  $^{20}\text{Ne}$  ions with energies per nucleon of 450 and 585 MeV have been most commonly used. The numbers of patients treated were 2054 patients with helium ion beams and 433 patients with neon ion beams. The patients treated with helium ions included primary skull base tumors: chondrosarcomas, chordomas, meningiomas, etc. The patient treated during 1987-1992 showed increased local control, representing the influence of improved immobilization, treatment planning and delivery, and availability of MRI. Using  $^{20}\text{Ne}$  ions, they also treated, and obtained excellent 5-year local control of, carcinomatous lesions arising from paranasal sinuses, nasopharynx or salivary glands, and extending into the skull base. Complications observed were mainly cranial nerve injuries including optic nerves, and radiation injury in the brain stem or temporal lobes.<sup>42</sup>

Since the end of 1997, clinical trials at the Gesellschaft für Schwerionenforschung (GSI), Darmstadt, have treated with carbon-ion beams relatively radioresistant tumors such as chordomas and low-grade chondrosarcomas of the skull base, adenoid cystic carcinomas and malignant meningiomas.<sup>43,44</sup> These tumors in the head region, which have not been treatable with conventional therapy methods. The new therapy led to a significant reduction of the tumor in all patients without any signs of relapse; local control rates achieved were comparable to neutron therapy but with less toxicity. By June 2005, about 250 patients have been treated successfully at GSI. Based on the studies at GSI, a therapy centre in Heidelberg is being built where up to 1,000 patients per year could be treated.

In 1994 the National Institute of Radiological Sciences (NIRS) in Chiba, Japan, commissioned its Heavy Ion Medical Accelerator in Chiba (HIMAC), which has two synchrotrons and produces ion beams from  $^4\text{He}$  to  $^{40}\text{Ar}$  up to a maximum energy per nucleon of 800 MeV. The HIMAC houses two treatment rooms, one with both a horizontal and a vertical beam, and the other with a vertical beam only. There are also a secondary (radioactive) beam room, a biology experimental room, and a physics experimental room, all equipped with horizontal beam lines. All beam lines are of the fixed beam type, in contrast to rotating gantries. Currently, their clinical trials use carbon ions, and they have successfully treated 1796 patients by February 2004. Currently, Phase I and II clinical trials are under way. They have demonstrated safety and efficacy of carbon ions to a great extent. In the near future they plan to establish an optimum irradiation method, identify the sites and histological types in which carbon ions are particularly effective, and clarify differences in indication from low-LET radiation. In 2004 HIMAC has obtained for the carbon-ion treatment the Japanese government

---

<sup>41</sup> J.R. Castro, J.M. Quivey, J.T. Lyman, G.T. Chen, T.L. Phillips, C.A. Tobias, and E.L. Alpen, "Current status of clinical particle radiotherapy at Lawrence Berkeley Laboratory," *Cancer* **46**: 633-641 (1980); J. Castro, *Progress in Radio-Oncology* (Ed. D Kogelnik), 643-648 (1995); J.R. Castro, "Clinical programmes: a review of past and existing hadron protocols," in *Advances in Hadrontherapy*, (U. Amaldi, B. Larsson, and Y. Lemoigne, editors), Excerpta Medica, Elsevier, International Congress Series **1144**: 79-94 (1997).

<sup>42</sup> J.R. Castro, D.E. Linstadt, J.P. Bahary, et al., "Experience in charged particle irradiation of tumours of the skull base: 1977-1992," *Int. J. Radia. Oncol. Biol. Phys.* **29**: 647 (1994).

<sup>43</sup> H. Eickhoff, T. Haberer, G. Kraft, U. Krause, M. Richter, R. Steiner, J. Debus, "The GSI Cancer Therapy Project," *Strahlenther. Onkol.* **175 (Suppl.2)**: 21-24 (1999).

<sup>44</sup> D. Schulz-Ertner, A. Nikoghosyan, C. Thilmann, Th. Haberer, O. Jäkel, C. Karger, G. Kraft, M. Wannemacher, J. Debus, "Results of carbon ion radiotherapy in 152 patients," *Int. J. Rad. Oncol. Biol. Phys.* **58**: 631 - 640 (2004).

approval as “highly advanced medical technology,” which is comparable to the US FDA approval.

In 2001 at Harima Science Garden City, Japan, the Hyogo Ion Beam Medical Center (HIBMC) was commissioned as the first hospital-based facility in the world to provide both proton and carbon-ion beam therapy, which provides protons of maximum energy of 230 MeV and carbon ions of maximum energy per nucleon of 320 MeV. Six therapy rooms are available with seven treatment ports. Three rooms are dedicated to carbon ion beams: one with a vertical beam line, one with a horizontal and one with a 45 degree oblique beam line. Two proton treatment rooms are equipped with commercially designed rotating gantries. By the end of 2005, HIBMC has treated 825 patients using protons and 53 patients with carbon-ion beams.

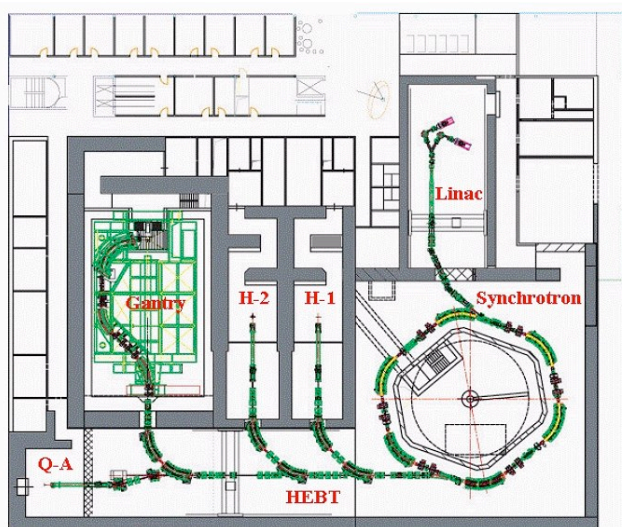


Fig. 14. Plan view of the Ion Therapy Unit under construction in Heidelberg.

The Heidelberg Ion Beam Therapy Center (HIT) is constructing the Ion Therapy Unit in Heidelberg, Germany. It is a joint project of the University Clinic Heidelberg, the German Cancer Research Center (DKFZ), the Gesellschaft für Schwerionenforschung (GSI) and the Research Center Rossendorf (FZR). As shown in Fig. 14, two ion sources feed the synchrotron via a linear accelerator. It houses three treatment rooms: two with a horizontal beam (H-1 and H-2) and one with a rotating gantry, which makes it possible to aim the beam at the patient from all directions. This system, which will be capable of treating tumors with both carbon ions and protons, is expected to begin treating patients in 2007.

European Network for LIGHT ion Therapy (ENLIGHT) plans for four national centers: Heidelberg Ion Therapy (HIT); the Centro Nazionale di Adroterapia Oncologica (CNAO) in Pavia; MedAustron in Wiener Neustadt; and ETOILE in Lyon. There is an increasing interest in further initiatives and more countries are expressing interest in creating national projects, in particular Sweden, the Netherlands, Belgium, Spain and the UK. There are other initiatives for light-ion facilities in several locations in the US and Japan, in Lanzhou, China, in Busan, Korea, and elsewhere.

## **Relation between the present report and other IAEA and ICRU reports**

The present report will be on “Dose and volume specification for prescribing, recording and reporting ion-beam therapy” –

- to help accurately administer treatments
  - for individual patient treatment
  - for therapy planning
  - for data management with DICOM compliance (IMPAC)
- to standardize the treatment reporting
- to facilitate meaningful inter-comparison of treatment results among carbon ion centers
  - also inter-comparison with conventional therapy

## **Issues to consider including in the present report:**

### **Prescribe and report doses to volumes rather than to discrete points**

- Justifications for it for carbon-ion treatment

### **The location/volume of the dose specification in treatment plan**

- The dose should be specified at the point where the dose changes least for small errors in determining ion beam path due to the uncertainties in integrated stopping power.
  - Mid-peak of the SOBP
  - Not at the proximal peak of the SOBP.
- The dose should be specified at the point where the dose changes most rapidly for small errors in determining ion beam path due to the uncertainties in integrated stopping power.
  - Mid-point of the distal dose falloff
- Dose-volume histogram

### **Units of dose specified and reported**

- “Physical dose and RBE” vs. “biological dose” in “Gray-equivalent (GyE)” (dose-weighting factors)

### **Should one specify the errors in treatment plans?**

- Errors help assess the under-dosing within the treatment volume, and over-dosing the adjacent normal tissues.<sup>45</sup>
- (Corollary) Should one present the upper and lower limits of dose delivered within a certain volume?

### **Are the radioactive beam measurements of dose delivery important?**

- It improves the accuracy of treatment planning and delivery.

### **Dose verification of treatment delivery**

- For scanned beam delivery, a measurement requires a complete scan of the entire field.
  - In case when a treatment is accomplished by assembling several non-uniform dose distributions, each dose measurement for verification requires complete scans. A very time- and accelerator resource-consuming process.
  - Multiple detectorss

### **Dosimetry standardization for inter-comparisons among ion-beam centers**

- Dosimeter calibrations
- Do you compare physical or biological doses?
  - What units for biological doses?
- Will it be practical, or feasible or even advisable, to agree on a “standard” ion beam setup with comparable beam quality? Weighting of absorbed dose implies the selection of reference treatment conditions.<sup>46</sup>

---

<sup>45</sup> M. Goitein, “Calculation of the uncertainty in the dose delivered in radiation therapy,” *Med. Phys.* 12: 608-612 (1985).

<sup>46</sup> A.Wambersie, R.Gahbauer and H.G.Menzel, “RBE and weighting of absorbed dose in ion-beam therapy,” *Radiotherapy and Oncology*, **73 (Suppl.2)**, 40-49, and 176-182 (2004); and A.Wambersie, H.G.Menzel, R.A.Gahbauer, D.T.L.Jones, B.D.Michael, H.Paretzke, “Biological weighting of absorbed dose in radiation therapy,” *Radiation Protection Dosimetry*, **99**: 445-452 (2002).